# Dynamic Clustering for Tracking Multiple Transceiver-free Objects

Dian Zhang
Department of Computer Science and Engineering
Hong Kong University of Science and Technology
Clear Water Bay, Kowloon, Hong Kong
zhangd@cse.ust.hk

Lionel M. Ni
Department of Computer Science and Engineering
Hong Kong University of Science and Technology
Clear Water Bay, Kowloon, Hong Kong
ni@cse.ust.hk

*Abstract*—RF-based transceiver-free object tracking, originally proposed by the authors, allows real-time tracking of a moving object, where the object does not have to be equipped with an RF transceiver. Our previous algorithm, the best cover algorithm, suffers from a drawback, i.e., it does not work well when there are multiple objects in the tracking area. In this paper, we propose a localization model of distance, transmission power and the signal dynamics caused by the objects. The signal dynamics are derived from the measured Radio Signal Strength Indication (RSSI). Using this new model, we propose the "probabilistic cover algorithm" which is based on distributed dynamic clustering thus it can dramatically improve the localization accuracy when multiple objects are present. Moreover, the probabilistic cover algorithm can reduce the tracking latency in the system. We argue that the small overhead of the proposed algorithm makes it scalable for large deployment. Experimental results show that in addition to its ability to identify multiple objects, the tracking accuracy is improved at a rate of 10% to 20%.

*Keywords- RSSI; Signal dynamics; Transceiver-free objects; localization; dynamic clustering*

## I. INTRODUCTION

Moving object tracking is important to many location-based applications and has attracted the attention of many researchers. Applications include: vehicle tracking [1] using GPS, enemy tracking using sensor networks in a battlefield [2], monitoring migration behavior of animals [4], and patient tracking inside the building of a hospital [5]. Traditional object tracking technologies can be divided into two categories: non-radio based and radio based. Non-radio based technologies usually employ video [14], infrared [15], ultrasound [9], and pressure [13] sensors. Typical radio-based object tracking methods require both target objects and reference objects to communicate with each other to collect Radio Signal Strength Indication (RSSI) information in order to estimate the position of nodes. These methods include GPS [17], 802.11 [16], active RFID [11], and RF-based wireless sensor networks [4] [10] [12]. All these methods require the target object to carry a transmitter, which periodically transmits beacon messages (e.g., active RFID tags), or a receiver to receive information from nearby transmitters (e.g., 802.11 detectors), or both (e.g., sensor nodes). Our work is based on radio technology in a

wireless network. However, to alleviate the requirement of carrying a transceiver by the target object, we were the first, to the best of our knowledge, to propose the idea of transceiver-free object tracking [3], where nodes to be localized do not have to carry a radio transceiver.

In our previous work [3], we proposed a signal dynamic model to capture the RSSI changing behavior due to the movement of objects. In our setup a wireless mesh network is established between sensor nodes, and the network determines the presence of object due to the variation in the signal levels between nodes. We then proposed the best-cover algorithm [3] to reach the localization accuracy of a single object to 0.99m in average based on the experiments with a 4×4 RF-based grid array covering 36 square meters. Our previous work has several drawbacks. First, the best cover algorithm does not work well with multiple objects. Second, the tracking latency was long: 3 seconds fixed. Third, the algorithm did not scale well to a large application area.

To alleviate the above practical drawbacks, in this paper, we propose the probabilistic cover algorithm based on a dynamic clustering, we named *Distributed Dynamic Clustering* (DDC). The basic idea behind DDC is to dynamically form a cluster of those wireless communication nodes whose received signal strengths are influenced by the objects. We argue that traditional fixed clusters [18] [19] proposed for other purposes in wireless sensor networks are not scalable to handle different objects with different impact areas. Dynamic clustering can overcome this problem and construct different clusters according to different objects. By using our model and a probabilistic methodology, we could more easily determine the number of objects in the area and locate them accurately. Moreover, by dynamically adjusting the transmission power when forming clusters, the interference between nodes will be reduced; this can further improve tracking accuracy.

The major contribution of this paper compared to our previous work lies in two aspects. First, we propose a new model for our radio nodes that considers both node distance and transmission power, in addition to signal dynamics. Thus, even for single object localization, the probabilistic cover algorithm provides improved localization accuracy. Second, we propose a distributed dynamic clustering method to allow the detection of multiple objects.
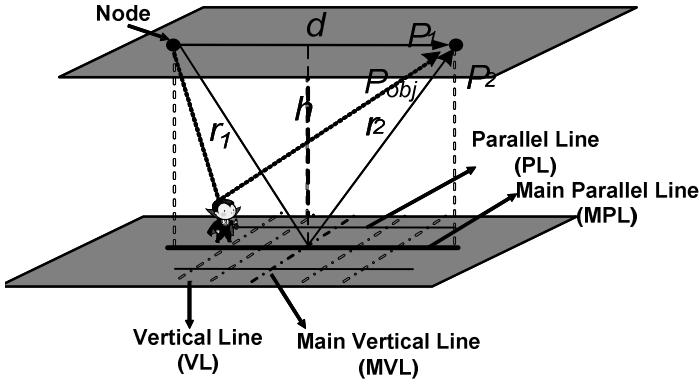
Figure 1: Position classification on the ground



Figure 2:    3D view of a signal dynamic test

The rest of this paper is organized as follows. In the next section, we discuss significant related work. Section III introduces the propagation model and presents the relationship between transmission power, wireless communication node distance and the signal dynamics. Then, the probabilistic cover algorithm is introduced in Section IV, followed by the experimental results and evaluation of the performance. Finally, Section VII concludes the paper and lists our future work.

## II.    RELATED WORK

Many radio-based technologies have been proposed to track mobile objects. Most of these RF technologies require the target objects to be equipped with a transceiver and thus we do not consider them in this section.

Passive IR [15] can record the number of people crossing a restricted area by monitoring the area's entry points. However, this approach requires dense deployment of such devices and is only sensitive to temperature changes and still requires a network on which data can be relayed. Ultrasound-based methods usually require target objects to carry an ultrasound transmitter or a receiver. For example, the target should carry a Bat (transmitter) in the Bat Ultrasound Location System [22]. Laser ranging [23] is famous for the accuracy of its distance measurement. However, the cost of such technology is usually prohibitive.

Research on transceiver-free object tracking based on RF technologies is in its infancy. The promise of this technology is in using the same radio network that relays location information in determining the location of objects tracked. There are only a few other works in this area. Device-free passive localization [6] examined the feasibility of using radio signal dynamics for object detection with two pairs of 802.11 transceivers. This work, however, only provided some raw data from the experiments. Neither real deployment nor real experimental results were reported.

From the RF propagation model aspect, there are many works that predict RSSI for a pair of transceivers, such as the free space model and the ground reflection model [20]. Most of these models just calculate the received power as a function of distance between the transmitter and receiver. However, none of these models considers how mobile transceiver-free objects affect the received power of the signal.
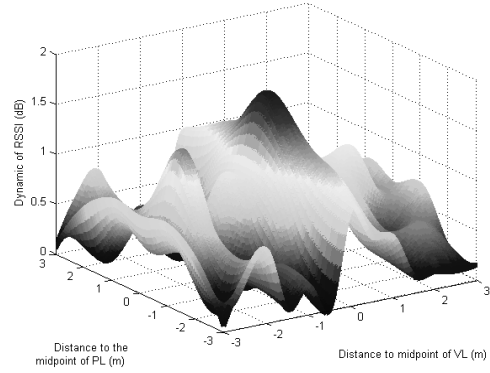
## III.    THE MODEL

In our previous work, we investigated the model of how the movement of a transceiver-free object will affect the signal strength between two communicating nodes [3]. In this paper, we extend our work and propose a more accurate model and describe the approaches of how we can estimate the possible object area for one pair of communicating nodes, which is based on RSSI dynamics and the position of the two nodes. Moreover, we also describe the relationship between node distance, transmission power and RSSI dynamics. The model offers a theoretical foundation for our methodology.

First, we review some definitions [3] and then illustrate how we estimate the possible object area.

### A.    Position classification on the ground

As shown **Figure 1**, if the nodes in the infrastructure are embedded in a building's ceilings, the position of the objects on the ground has the following descriptors:

- The *main parallel line* (MPL) is the ground projection of the transmitter-receiver line.

- The *main vertical line* (MVL) is perpendicular in the ground plane to the MPL, crossing the midpoint of the MPL.

- *Parallel Lines* (PL) are on the ground plane, parallel to the MPL (including the MPL).

- *Vertical Lines* (VL) are on the ground plane, parallel to the MVL (including the MVL).

### B.    Environment Definition

- In a *static environment*, environment factors such as temperature and humidity are kept unchanged and there are no moving objects in the environment.

- In a *dynamic environment*, an object moves into a static environment.

- *Signal dynamics* describe the fluctuations and differences in the RSSI between the static and the dynamic environments.
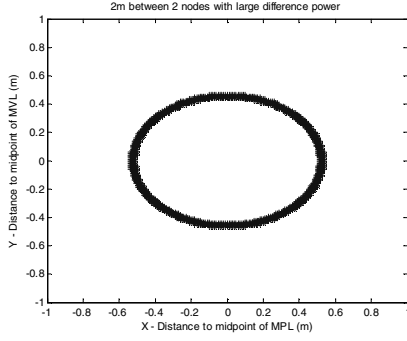
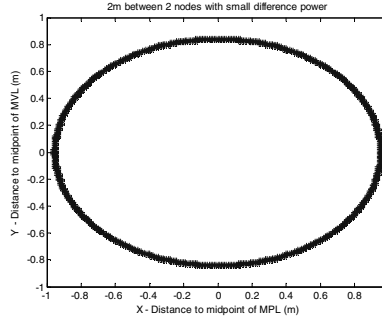Figure 3: The possible object area with a large power difference

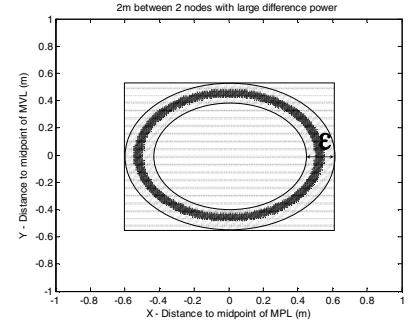Figure 4: The possible object area with a small power difference

Figure 5: The possible object area with an error bound

## C. Properties of Signal Dynamics

Along each PL or VL, if the object's position is closer to the line's midpoint, the RSSI changes caused by the object are larger. This is shown in **Figure 2**, where we measured the RSSI change caused by a moving object versus the distance of the object from such midpoints.

In our previous work, we also observed and proved that when the object's position is on the MPL or MVL, the RSSI dynamics are much larger than if the object is at a comparable location on any other PLs or VLs [3]. Therefore, in our new model test, we restrict our test to object positions on the MPL or the MVL.

## D. Possible Object Area Calculation

In our previous paper we proved that the difference in power received by the receiver between the static and dynamic environments is as below.

$$\Delta P \approx P_{obj} \qquad (1)$$

$P_{obj}$ is the received power influenced by the target object according to radar equation [7],

$$P_{obj} = \frac{P_t G_t \, G_r \lambda^2 \sigma}{(4\pi)^3 r_1^2 r_2^2} \qquad (2)$$

Thus:

$$r_1 r_2 = \sqrt{\frac{P_t G_t G_r \lambda^2 \sigma}{(4\pi)^3 P_{obj}}} \approx \sqrt{\frac{P_t G_t G_r \lambda^2 \sigma}{(4\pi)^3 \Delta P}} \qquad (3)$$

Here,

- $r_1$ is the distance from the transmitter to the target object on the ground.

- $r_2$ is the distance from the target object on the ground to the receiver.

- σ is the radar cross section of the target object, it is defined as the ratio of scattered power to incident power density. According to [7], its value for a human being is 1.

- $P_t$ is the transmitted power in watts, according to [7]

$$P_t = 0.001 * 2^{\ dBm/10} \qquad (4)$$

0 dBm is corresponding to 1 mw.

- $G_t$, $G_r$ are the transmitter and the receiver antenna gain respectively. Both of these parameters are fixed, since they are measures of how much more sensitive an antenna is over an isotropic antenna [7] and each MICA2 node in our experiments has the same fixed antenna.

- $\lambda$ is the radio wavelength in meters. In our experiments it is about 0.345 m, which is calculated as the ratio of the speed of light and the employed frequency (which is 870MHz in our experiments).

- $d$ is the distance from the transmitter to receiver. This is fixed for each pair of nodes after the deployment.

Therefore, all the parameters above have fixed values for a fixed pair of nodes (assuming that one type of object is being localized). $\triangle P$ can also be calculated according to the RSSI data in the static environment and dynamic environment for the MICA2 nodes:

$$\text{dBm} = (\text{-50*RSSI*1.223}/V) \text{ - 45.5} \qquad (5)$$

where $V$ is the battery voltage of the node.

We assume that for each pair of nodes and each time it receives data from which RSSI can be extracted, $r_1 r_2$ is a constant (i.e., objects' speeds are significantly less than the speed of light).

As shown in **Figure 3** and **Figure 4**, the possible object area in a perfect environment is on the border of an ellipse (projected to the ground). When $\triangle P$ is larger, $r_1 r_2$ is smaller, thus the ellipse is also smaller, and vice versa for smaller $\triangle P$. Moreover, if we consider some error bound ε, the possible object area on the ground becomes a hollow ellipse as illustrated in **Figure 5**. In order to describe this area more easily, we employ a bounding rectangle over the ellipse, and thus the area of the rectangle is an upper bound of the possible object area.

## E. Experimental Setup

In our experiments, we use MICA2 sensor nodes with Chipcon CC1000 radio transceiver chips [8]. The radio frequency is 870 MHz. MICA2 use a custom tailored TinyOS
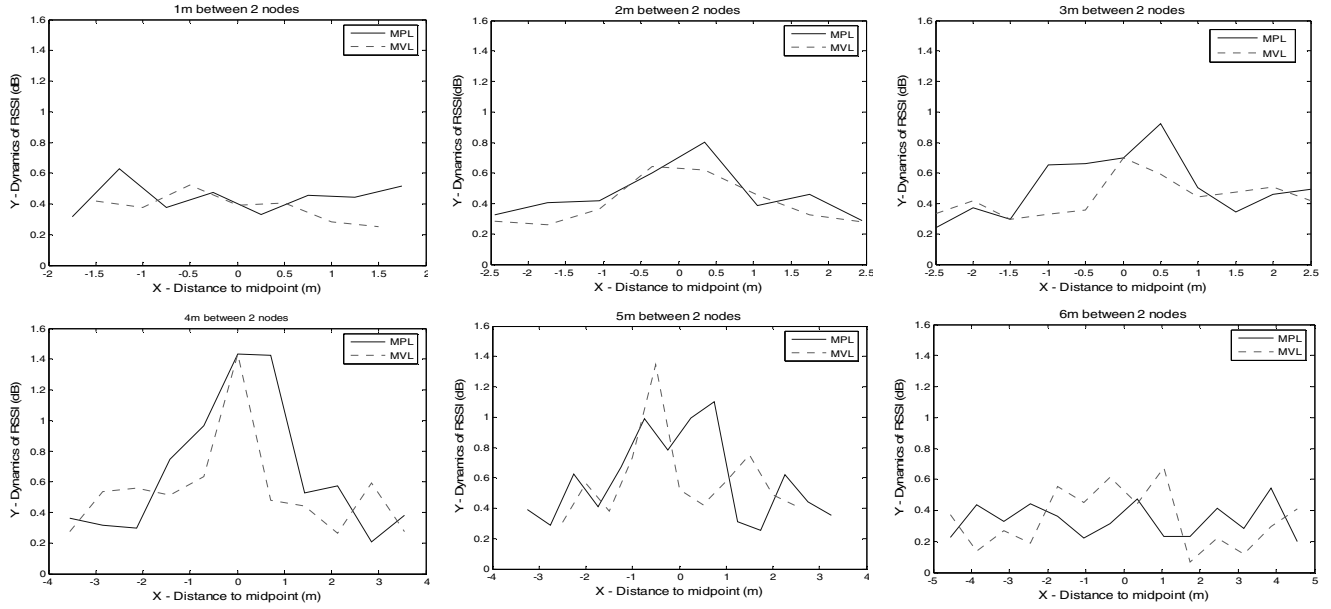
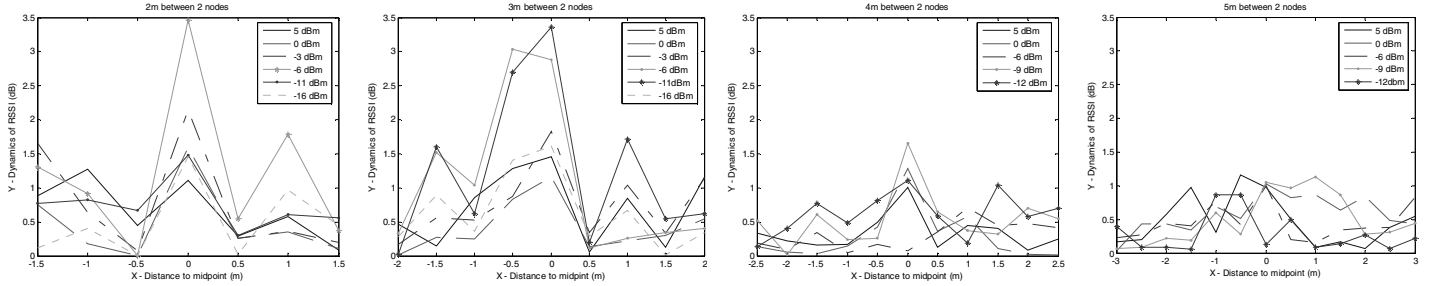Figure 6: Relationship between distance and signal dynamics on different node distances



Figure 7: Relationship between transmission power and signal dynamics on different node distances

[21] operating system.

## F. *Relationship between Node Distance and Signal Dynamics*

We first conducted a test on the relationship between infrastructure node distance and signal dynamics when the object is at different positions on the MPL and the MVL. After testing different node distances from 1m to 6m, we verified that different node distances cause different RSSI dynamic behaviors, as shown in **Figure 6**. We also found that the dynamic behavior is not obvious when the node distances are below 1m and above 6m. In the latter cases we cannot experience a "bump" at the center part. This is because for the short node distance, the received signal strength is very strong especially for the short line-of-sight radio propagation path, and it is not easily influenced by the scatted wave caused by the object. On the other hand, for large node distance, the received signal strength is too weak and is easily influenced by noise and other interference.

## G. *Relationship between Transmission Power and Signal Dynamics*

In order to determine how much the transmission power will affect the signal dynamics of two communicating nodes, we use a person to represent the object standing on different positions of the MPL line. We test 26 levels of transmission

powers from -20 dBm to 5 dBm with node distances ranging from 2m to 5m (based on arguments of our previous experiment).

Experimental results show that for most transmission levels, the dynamic behavior is significant. That is, the dynamics "bump up" around the center of MPL. As the transmission powers sink lower and/or node distances becomes larger, the received signal strength is very weak and is susceptible to noise interference. For example, when the node distance is 2m or 3m, the dynamic behavior is not obvious if the transmission power is less than -16 dBm. Similarly, when the node distance is at 4m or 5m, the dynamic behavior is not obvious if the transmission power is less than -12 dBm.

We also found that when the distance is 2m or 3m, the signal dynamic behavior grows larger as the transmission power goes down (i.e., transmission power should be set slightly above the lower threshold). A transmission power from -6 dBm to -11 dBm has the most significant dynamics at these distances. After that, the signal dynamic behavior is reduced. However, when the node distance is 4m or 5m, the dynamics do not change much with the adjustment of transmission power (i.e., the transmission power cannot be raised enough to see the previous effect). Thus if the node distance is not very large, there is a *sensitive transmission power* range that causes the biggest signal dynamics.
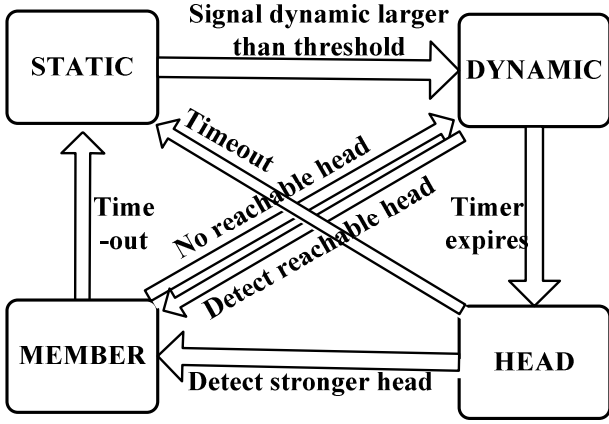
Figure 8: Four states of event nodes in distributed dynamic clustering

In our previous work, we used 0 dBm as the default transmission power. If we reduce the transmission power to the *sensitive transmission power* range, we can have higher dynamic values for short node distances. In our experiments, according to **Figure 7**, sensitive transmission power can cause the dynamic signal value to increase by about a factor of two. Moreover, the inter-nodal interference can be reduced through reducing the transmission power, thus transmissions from nodes that are not used for the current calculation create less interference, which can potentially improve tracking accuracy.

## IV. LOCATION ESTIMATION METHDOLOGY

In our test deployment, we place a wireless communication node grid on the ceiling of a room (**Figure 11**). Each node functions both as a transmitter and as a receiver. According to our model, we term *influential links* those wireless links whose signal dynamics between static environment (no tracking objects) and dynamic environment (with tracking objects) are larger than a threshold [3]. Such influential links will tend to be clustered around the tracked objects. Our basic idea is to form different clusters based on the influential links and use such information to locate single or multiple objects.

In this section, first we propose the *Distributed Dynamic Clustering* method to identify the clusters of nodes. If multiple objects are not very close to each other, this algorithm can dynamically form different clusters for multiple objects. Also, instead of each node transmitting information on all these events back to the gateway for further processing, we use a distributed approach to identify the nodes located near each object and choose one node having the greatest remaining energy to be the cluster head. Each cluster head gathers local information about the signal dynamics of those influential links associated with those nodes within one hop. Then, we will employ the probabilistic cover algorithm at the cluster head pre-processing local information before sending the result back to gateway.

### A. Distributed Dynamic Clustering (DDC)

This method aims at clustering the sensor nodes associated with the influential links, which are close to the objects. Multiple objects may cause multiple different clusters. This dynamic clustering mechanism is distinguished from other

clustering work due to the short life time of clusters. The life time usually starts when influential links are detected and ends after the local information have been collected in the cluster head.

In DDC, each node has four states; the relationship of states is depicted in Figure 8. At the beginning, all nodes are in the STATIC state. Each node builds a static table to store the static RSSI values for its neighbors after receiving beacons from neighbors. Nodes ignore packets transmitted from nodes beyond five meters (as explained in Section III). The link thresholds are computed from these static RSSI values. When a node measures its received RSSI dynamic value larger than the threshold, it enters DYNAMIC state and starts an initial timer, signifying an *event detection*. The purpose of having an initial timer is to prevent more than one node in the next step from declaring themselves to be cluster heads at the same time (reducing communication overhead). The initial timer on node $i$ at time $t$ is defined in Equations 7 and 8.

$$t^i_{init(t)} = (1 - p^i_t) \times T_c + t_r \qquad (7)$$

$$p^i_t = \frac{V^i_t - V_{min}}{V_{max} - V_{min}} \qquad (8)$$

$p^i_t$ is node $i$'s remaining power described as the percentage over the node's initial power. We approximate the remaining energy by real-time voltage data which can be directly read from ADC readings in TinyOS. $V_{max}$ is 3.0V for a two AA battery powered sensor platform. $T_c$ is a constant, which causes low energy nodes to wait at least $T_c$. $T_c$ should be defined according to the transmission time of a single packet and the size of the cluster. In our experiments, we set $T_c$ to half a second. $t_r$ is a small random timer upper bound by $T_c$. By using this setting, we can force that the strongest node in each cluster will declare itself to be the cluster head.

During DYNAMIC state, the node will become a member node when it detects a reachable head. Otherwise, it will claim itself as a cluster head and enters the HEAD state after the timer expires. When a head node discovers a stronger head candidate within its reach (on hop away), it will transition into the MEMBER state and associate itself with the stronger head. If two nodes have the same remaining energy measure, node IDs will be used to break the tie. The head selection criteria will guarantee that the strongest node will be selected as the head. The head node also has the information of the influential links in its cluster. It should be noted that one MEMBER node can associate with more than one HEAD node. In other words, different clusters may incidentally overlap.

### B. Probabilistic Cover Algorithm

After the head is chosen, it will use the signal dynamics information on the influential links from neighbors to estimate the object's position. The basic idea behind the probabilistic cover algorithm is to estimate a possible object area for each influential link base on our model. As there may be many influential links many such areas will be created. Based on these areas, a probabilistic method is used to obtain the final estimated object position.
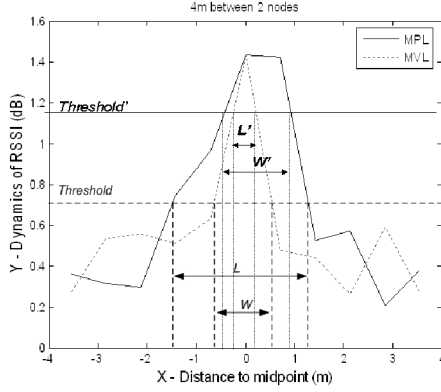
Figure 9: An example of calibration on different node distances



Figure 10: The probabilistic cover algorithm

As explained in Section III, for each influential link, the actual possible object area should be like an ellipse, but to easy the burden of calculation we use a bounding rectangle to represent it. In order to get the size of the rectangle, we use a dynamic threshold to intercept the dynamic lines of such link. The interval on MPL is set as the length of the rectangle such as *L* or *L'*. The interval on MVL is set as the width of the rectangle such as *W* or *W'*. If the value of the dynamic threshold is high, the possible object area will be small, and vice versa. Figure 9 is one example where we used a node distance of 4 meters. The solid line represents the dynamics on the MPL and the dashed line represents the dynamics on the MVL.

For each influential link with a different distance, we can obtain the size of the rectangle. For each rectangle, we set a weight value to represent the possibility that the object is in this area.

$$Pr_i (\%) = D / M_i \qquad (6)$$

Here, $Pr_i$ is a percentage to represent the possibility that the object is in the calculated area for the influential link $i$. $D$ is the received RSSI dynamic and $M_i$ is the average maximum dynamics retrieved in the model for the influential link $i$. Moreover, according to the model, the weight for shorter node distances should be higher than that for longer node distances if the transmission power is adjusted to the *sensitive transmission power*.

After estimating the possible object area on each influential link, in the node grid there will be many such rectangles as shown in Figure 10. Rectangle $i$ will have a weight value of $Pr_i$ and some of these rectangles will overlap. If one location has more overlapping rectangles with higher weight, the object is more likely to be within that area. There may be several rectangle clusters in the area caused by either other objects or by noise. We ignore those clusters with small number of rectangles due to the high probability that they are caused by noise. The probabilistic cover algorithm is applied to each cluster. We use a fixed square area to scan in the cluster (to be described later). At each scanning step, we calculate the sum of the weights of the rectangles that are intersecting with the square, and then select the position with the largest sum.
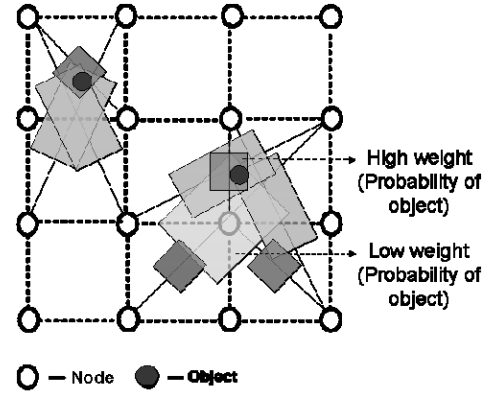
## V. IMPLEMENTATION

The proposed tracking system is implemented on MICA2 nodes with Chipcon CC1000 radio transceiver chips at 870MHz and monopole antennas [8]. We connect one MICA2 node to a notebook via a MIB520 [8] programming board to act as the sink. All other nodes are deployed on the of our test environment's ceiling (2.40 meters above the floor). Each node acts as both transmitter and receiver.

Our experiments are divided into two parts: model test and tracking test. The model test is performed separately in two similar rooms with similar area of about 12×9 square meters, as shown in Figure 11. During the model test, we examined one pair of nodes and aim at getting the relationship between its distance, transmission power and signal dynamics (we used these results when describing our model). So we can choose the best node distance and most sensitive transmission power for the following tracking.

The nodes in the tracking experiment are set up as a 4×4 node grid on the ceiling. The node distance is chosen as 2m so that we can ensure the most number of valid links in the grid setting [3]. The default transmission power is set as -10 dBm, which belongs to the sensitive transmission power range. In order to reduce beacon collisions, each node is required to wait a short random time before broadcasting a beacon. Since we have a relative low transmission power, we choose the initial beacon interval as 0.5 seconds. Each node performs the DDC algorithm, i.e., at first, each node is in the STATIC state. If objects come into the test area and the node's received signal strength is larger than a threshold, it enters DYNAMIC state. Through using the head selection criteria, the HEAD nodes will be selected, and it will gather the neighbor information and use the *Probabilistic Cover Algorithm* to calculate the object position. Then results are transmitted back to the sink for final processing. If nodes time-out and no more significant signal changes are detected then HEAD nodes transition back to the STATIC state.

## VI. PERFORMANCE EVALUATION

In this section, we compare the probabilistic cover algorithm with our previous best cover algorithm [3]. The comparisons consider both the cases of single and multiple
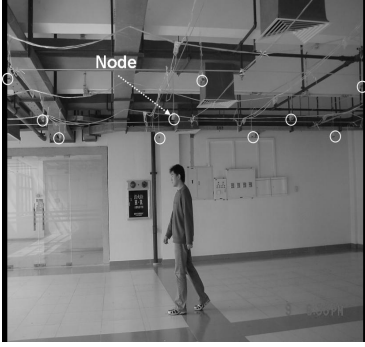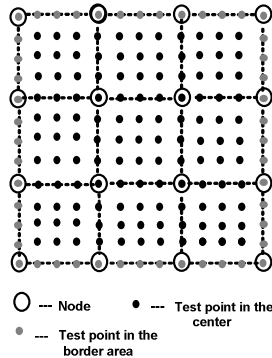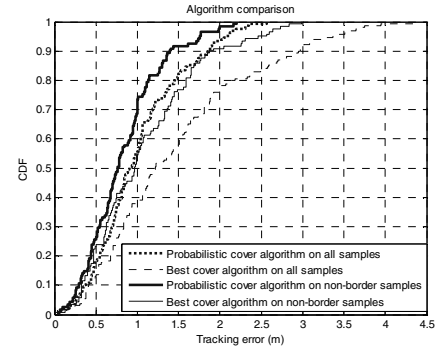
Figure 11: Experimental environment



O --- Node    ● --- Test point in the center
● --- Test point in the border area

Figure 12: Tested samples



Figure 13: Algorithm comparison of single object



□—Node □—Calculated Position    ∷—Object Position
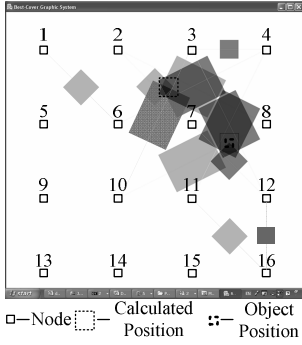
Figure 14: Single object test with the best cover algorithm



□—Node □—Calculated Position    ∷—Object Position
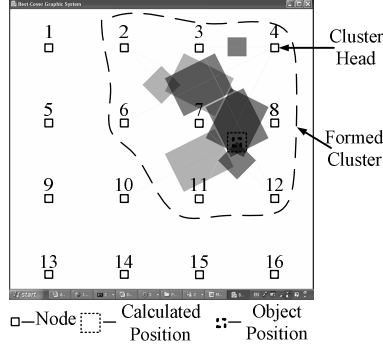
Figure 15: Single object test with the probabilistic cover algorithm



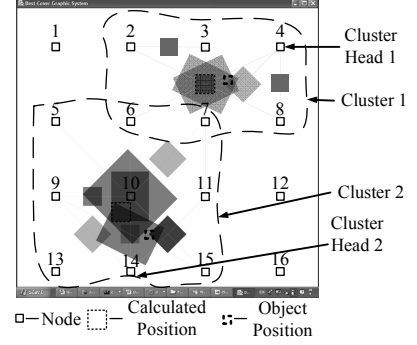□—Node □—Calculated Position    ∷—Object Position

Figure 16: Multiple objects test with the probabilistic cover algorithm

objects.

## A. Comparison of Algorithms on a Single Object

Based on 169 tested object position samples on the ground (with 48 of them on the border area) as Figure 12 shows, we compare our probabilistic cover algorithm with the best cover algorithm. The average tracking error of each algorithm is shown in Figure 13. We find that the tracking error is improved by a factor of about 10% for non-border samples, while for border samples this improvement can be greater than 20%. For non-border samples, the average tracking error can be reduced to 0.85m.

Figure 14 shows one example of the object position estimated by best cover algorithm, where the tracking error is 2.25m. Figure 15 shows the same example but when using the probabilistic cover algorithm. We can see that in DDC node 4 is selected as the cluster head as it has the strongest remaining power among the nodes which detect signal dynamics larger than the threshold. For a pair of nodes associated with one influential link, if one of these two nodes is not within one hop to the cluster, the head does not take it into consideration. We can see that the distance between node 10 and cluster head node 4 is larger than 5m. Thus, head node 4 will not count the influential links associated with node 10. Therefore, the cluster is smaller than that of the best cover algorithm and so localizes the object more easily with better accuracy. The tracking error of this example was 0.02 m.

In summary, the probabilistic cover algorithm provides a good improvement over the performance of the best cover algorithm, especially when target objects are on the border area.

## B. Tracking Multiple Objects

When there are multiple objects in the target area, as long as the objects are not tightly close to each other, the DDC method can easily separate them into different clusters. Within each cluster, the probabilistic cover algorithm is used to localize each object. In our experiments, we tested 20 different scenarios with two persons acting as moving objects (as shown in Figure 12). The average distance between the two persons is about 5m. Experimental result show that in 18 out of the 20 cases we can differentiate between the two distinct objects, while the best cover algorithm can only differentiate them in 5 out of the 20 cases. The localization accuracy with DDC on average is 1.08m.

Figure 16 shows a sample example of the multiple object experiments. In this example, two clusters are formed by using DDC. It is worth mentioning that node 6 and node 7 belong to both clusters. They will send the received signal dynamics to both cluster heads.

Because the probabilistic cover algorithm has a smaller cluster size than that of the best cover algorithm, it is much easier for the probabilistic cover algorithm to localize multiple objects. We can empirically conclude that the probabilistic cover algorithm will perform best if the distance between the multiple objects is larger than five meters and the deployment area is large.

## C. Latency

When employing our DDC method for tracking, we have two major types of delay. The first type of delay is the

broadcast interval of beacons. Since there are contentions in the broadcast channel, the broadcast interval is determined by the density of the nodes and the transmission power of each node. As we reduced the transmission power of each node down to 10 dBm, the number of nodes within one cluster will be smaller. Therefore, we may reduce the time interval for sending beacon messages of each node much less than 3 seconds as used in our previous method [3]. In our DDC experiments, we set the beacon interval as 1 second. Moreover, we could dynamically adjust the beacon intervals according to the signal dynamic it receives. If it is larger, the beacon interval is smaller, and vice versa.

The second type of delay is the initial timer in the algorithm for turning a node from DYNAMIC state into HEAD state. As we described before, this value in our experiments is initially set around 0.5 seconds and cannot be larger than 1 second.

To summarize, the probabilistic cover algorithms has smaller latency to totally about 2 seconds and low overhead, making it scalable for large deployment.

## VII. CONCLUSIONS AND FUTURE WORK

In this paper we proposed the probabilistic cover algorithm to track multiple transceiver-free objects based on RF technologies. Based on the model and the relationship between node distance, transmission power and signal dynamics caused by the transceiver-free objects, our approach can calculate the possible object area for each pair of wireless communicating nodes. After that, we use *distributed dynamic clustering* to track multiple objects. The intention of clustering tries to divide the events created by moving objects into clusters. In each cluster the probabilistic cover algorithm is used to calculate the object position. As long as the objects are not too tightly close to each other, the algorithm can differentiate between them. Moreover, we have shown that the probabilistic cover algorithm can reduce the tracking latency. The small overhead of the proposed algorithms makes them more scalable for large deployment.

Our approach to multiple moving objects still has some limitations when multiple objects cross each other's trajectory. We need to develop probabilistic models to analyze the dynamic behavior of such multiple moving traces. Furthermore, we intend to investigate the impact of employing different frequencies when determining the signal dynamics. In the future we will also consider different topologies when deploying communicating nodes.

## REFERENCES

[1] Advanced Tracking Technologies, Inc., http://www.a dvantrack.com.

[2] Rockwell Scientific Company, http://wins.rockwells cientific. com/

[3] D. Zhang, J. Ma, Q. Chen and L. M. Ni, "An RF-based system for tracking transceiver-free objects," in Proceeding of the 5th annual IEEE International Conference on Pervasive Computing and Communications, 2007.

[4] P. Juang, H. Oki, Y. Wang, M. Martonosi et al., "Energy-Efficient Computing for Wildlife Tracking: Design Tradeoffs and Early Experiences with ZebraNet," in Proceeding of the 10th International Conference on Architectural Support for Programming Languages and Operating Systems (ASPLOS-X), 2002.

[5] T. Gao, D. Greenspan, M. Welsh, R. R. Juang, and A. Alm, "Vital signs monitoring and patient tracking over a wireless network," in Proceedings of the 27th IEEE EMBS Annual International Conference, 2005.

[6] M. Youssef, M. Mah and A. Agrawala, "Challenges: device-free passive localization for wireless environments," in Proceedings of the 14th Annual International Conference on Mobile Computing and Networking, 2007.

[7] D. Pozar, "Microwave engineering," in 2nd ed., John Wiley and Sons, Inc., 1998.

[8] XBOW Corporation, "XBOW MICA2 mote specifications," http://www.xbow.com.

[9] P. Bahl, and V. N. Padmanabhan, "RADAR: an in-building RF-based user location and tracking system," in Proceedings of the Nineteenth Annual Joint Conference of the IEEE Computer and Communications Societies, 2000.

[10] D. Moore, J. Leonard, D. Rus, and S. Teller, "Robust distributed network localization with noisy range measurements," in Proceedings of the Second international conference on Embedded networked sensor systems, 2004.

[11] L. M. Ni, Y. L. Liu, Y. C., and A. P. Patil, "LANDMARC: indoor location sensing using active RFID," in Proceedings of the First IEEE International Conference on Pervasive Computing and Communications, 2003.

[12] D. Niculescu and B. Nath, "Ad hoc positioning system (APS) using AOA," in Proceedings of IEEE the Conference on Computer Communications, 2003.

[13] J. O. Robert and D. A. Gregory, "The smart floor: a mechanism for natural user identification and tracking," in Proceedings of the CHI 2000 Conference on Human Factors in Computing Systems, 2000.

[14] Q. Cai and J. K Aggarwal, "Automatic tracking of human motion in indoor scenes across multiple synchronized video streams," in Proceedings of the Sixth International Conference on Computer Vision,1998.

[15] ACOREL Corporation, http://www.acorel.com.

[16] J. Yin, Q. Yang, and L. M. Ni., "Adaptive temporal radio maps for indoor location estimation," in Proceedings of the Third IEEE International Conference on Pervasive Computing and Communications, 2005.

[17] G. Xu, "GPS: Theory, Algorithms and Applications," in Berlin: Springer-Verlag, 2003.

[18] Q. Chen, J. Ma, Y. Zhu, D. Zhang, L. M. Ni, "An Energy-Efficient K-Hop Clustering Framework for Wireless Sensor Networks," in Proceedings of 4th European Conference on Wireless Sensor Networks, 2007.

[19] S. Bandyopadhyay and E.J. Coyle, "An Energy Efficient Hierarchical Clustering Algorithm for Wireless Sensor Networks," INFOCOM, 2003.

[20] T. S. Rappaport, "Wireless communications: principles and practice," 2nd ed. Upper Saddle River, NJ: Prentice Hall PTR, 2002.

[21] Berkeley, http://www.tinyos.net.

[22] Cambridge, http://www.cl.cam.ac.uk/research/dtg/attarchive/bat/.

[23] R. Dorsch, G. Hausler, J. Herrmann, "Laser triangulation: fundamental uncertainty in distance measurement ",Applied OPTICS, vol. 33, No. 7, 1994.